J Therm Anal Calorim
DOI 10.1007/s10973-016-5956-y

Thermal and structural characterization of copper(II) complexes with phenyl-2-pyridylketoxime (HPPK)

R. Szczęsny[1] · E. Szłyk[1] · A. Kozakiewicz[1] · L. Dobrzańska[2]

Received: 12 August 2016 / Accepted: 8 November 2016

Abstract Copper(II) complexes of different nuclearity with phenyl-2-pyridylketoxime (HPPK), such as mononuclear [Cu(HPPK)(PPK)X], whereby $X = NCS^-$ **(1)** or NO_3^- **(2)**, dinuclear $[Cu(HPPK)Cl_2]_2$ **(3)** and trinuclear $[Cu_3(PPK)_3(\mu_3\text{–}OH)(Cl)_2]\cdot nH_2O$ **(4)** were synthesized, and their thermal properties were investigated. The studies involved gas-phase monitoring of decomposition products by infrared spectroscopy. Thermal decomposition performed in air revealed the multi-stage character of the process, the course of which depends on the compound composition. In all cases, CuO was found as the final product of the process. Furthermore, the crystal structure of **1** was revealed. It shows a square-pyramidal geometry around Cu(II), with the NCS^- ion situated in the apical position and two HPPK ligands present in the base, one of which is deprotonated.

Keywords Cu(II) complexes · Phenyl-2-pyridylketoxime · Thermal properties · SCXRD

Introduction

The chemistry of metal complexes with oxime type of ligands has been investigated from the 1960s of the twentieth century due to their applications as analytical reagents [1–4]. Currently, a renewed interest in this class of compounds can be observed, as they are being used for the design of homo-/heterometallic clusters [5], as well as coordination polymers with attention-grabbing properties [6]. In general, ketoxime-based metal complexes show potential for the development of new oxygen activation catalysts and interesting magnetic properties [7–10]. More in particular, copper complexes of phenyl-2-pyridylketoxime are known for the formation of trinuclear clusters, which are the inorganic structural and functional analogs of crown ethers, and display interesting magnetic behaviour [11, 12]. Some selective Ba^{2+} and Ca^{2+} receptors, based on site-selective transmetallation of polynuclear zinc(II)/polyoxime complexes, have been discovered [13]. Furthermore, copper oximes can be utilized as suitable model compounds of the biologically active sites that can interact either covalently or non-covalently with DNA [14].

Despite the broad literature on the behaviour of copper complexes with phenyl-2-pyridylketoxime in solution, the number of reports concerning the solid state is rather limited and mostly treating about the trinuclear compounds mentioned above. Recently, we presented for the first time some structures of mononuclear Cu(II) complexes with HPPK [15]. It is worth noting that in each case one of the HPPKs, constituting these mononuclear complexes, was found deprotonated, whereas in the case of mononuclear Ni(II), Mn(II) and Cd(II) complexes, the HPPK ligands are neutral. In all mononuclear complexes, HPPK shows an *N*,*N*′-chelating coordination mode involving both the nitrogen atom of the oxime group and the nitrogen atom of

Electronic supplementary material The online version of this article (doi:10.1007/s10973-016-5956-y) contains supplementary material, which is available to authorized users.

✉ R. Szczęsny
roszcz@umk.pl

[1] Faculty of Chemistry, Nicolaus Copernicus University in Toruń, 87-100 Toruń, Poland

[2] Crystal Engineering Laboratory, Centre of New Technologies, University of Warsaw, S. Banacha 2c, 02-097 Warsaw, Poland

Published online: 20 December 2016

the pyridyl group. However, depending on the pH and deprotonation level [1, 16], coordination via the oxygen atom is also feasible, leading to the formation of higher nuclearity compounds, whereby the composition of the final product depends on many other factors, such as metal ion, counterions and molar ratio [17–19].

Studies focusing on the thermal behaviour of HPPK metal complexes are also rare to come by. There are some reports treating about the thermolysis of other types of transition metal complexes with oximes [20–22], but once again, excluding our recent results [15], there is no literature on the thermal behaviour of Cu(II) complexes with phenyl 2-pyridylketoxime. In continuation of our studies on this family of compounds, aimed towards the selection of precursors for the low-cost fabrication of semiconducting CuO thin films, we would like to report our preliminary results on the decomposition process in air for a range of Cu(II) complexes, monitored by IR spectroscopy.

Experimental

Measurements

Thermal studies (TG, DTG, DTA) were performed on a SDT 2960 TA analyser. Decomposition processes were studied in dynamic atmosphere of dry air flowing at 40 mL min^{-1} with a heating rate of 10 and 5°C min^{-1} and a heating range up to 1000 °C (sample mass varied between 2 and 5 mg). Gaseous products of thermal decomposition were detected by a FT-IR Bio-Rad Excalibur spectrophotometer equipped with a thermal connector for gases evolved from a TA SDT 2960 analyser. IR spectra were registered with a PerkinElmer 2000 FT-IR spectrometer in the range of 4000–400 cm^{-1} for KBr discs. Powder X-ray diffraction (PXRD) analysis was performed using a Philips (Almelo, The Netherlands) XPERT θ–2θ diffractometer with CuKα radiation. Elemental analyses were performed on a Vario MACRO CHN apparatus (Elementar Analysensysteme GmbH).

Single-crystal X-ray crystallography

The single-crystal X-ray diffraction data for **1** were collected on an Oxford Sapphire CCD diffractometer, MoKα radiation (λ = 0.71073 Å). The CrysAlis package of programs was used for the data collection (CrysAlis CCD) [23], cell refinement and data reduction (CrysAlisPro Red) [24]. Empirical absorption correction was applied. The structure was solved by direct method using SHELXS-97 and refined by full-matrix least square method based on F2 using SHELXL-97 [25]. The program Mercury was used to prepare the molecular graphics image [26]. All non-hydrogen atoms were refined anisotropically, and the hydrogen atoms were placed in calculated positions with displacement factors fixed at 1.2 times Ueq of the parent C, O atoms with C–H = 0.95 (aromatic) and O–H = 0.82 Å. One of the phenyl rings (C25–C30) was found disordered over two positions with refined site occupancies of 0.59(2):0.41(2). Consequently, a few geometrical restraints were placed on the bond lengths of this ring. Details of the diffraction experiment and structure refinement are summarized in Table 1. CCDC-975557 (for **1**) contains the supplementary crystallographic data for this paper. These data can be obtained free of charge from The Cambridge Crystallographic Data Centre via www.ccdc.cam.ac.uk/data_request/cif.

Attempts were undertaken to determine the crystal structure of **2**; however, the poor quality of the crystals did not allow for full characterization. It was shown that it crystallizes in the *Fdd*2 space group of an orthorhombic system with unit cell parameters: $a = 34.7$ Å, $b = 29.2$ Å, $c = 8.9$ Å. The crystal structures of the two other compounds (**3** and **4**) have previously been described [27, 28].

Table 1 Crystal data and structure refinement parameters for **1**

Compound reference	**1**
Chemical formula	$C_{25}H_{19}CuN_5O_2S$
Formula mass	517.05
Crystal system	Monoclinic
a/Å	17.3809(6)
b/Å	8.6465(2)
c/Å	17.4403(5)
α/°	90.00
β/°	115.544(4)
γ/°	90.00
Unit cell volume/Å^3	2364.81(12)
Temperature/K	293(2)
Space group	$P2_1/c$
No. of formula units per unit cell, *Z*	4
Radiation type	MoKα
Absorption coefficient, μ/mm^{-1}	1.044
No. of reflections measured	13,431
No. of independent reflections	4797
R_{int}	0.0303
Final R_1^a values ($I > 2\sigma(I)$)	0.0396
Final $wR(F^2)^b$ values ($I > 2\sigma(I)$)	0.1054
Final R_1^a values (all data)[a]	0.0492
Final $wR(F^2)^b$ values (all data)	0.1115
Goodness of fit on F^2	1.040

[a] $R_1 = \sum||F_o| - |F_c||/\sum|F_o|$; [b] $wR_2 = \{\sum[w (F_o^2 - F_c^2)^2]/\sum[w (F_o^2)^2]\}^{1/2}$

Synthesis

[Cu(HPPK)(PPK)(SCN)] ***(1)****, [Cu(HPPK)(PPK)(NO$_3$)]* ***(2)*** *and [Cu(HPPK)Cl$_2$]$_2$* ***(3)***

Compounds **1–3** were synthesized as presented earlier [1, 29]. It was found that the compounds take up water over time, which might explain some discrepancies in the elemental analyses (the expected results are given, taking into account the presence of 0.5 water molecule for each compound as well). *Anal*. Calc. for $C_{25}H_{19}CuN_5O_2S$ **(1)**: C, 58.1; H, 3.7; N, 13.5. (with 0.5 H_2O: 57.1, 3.8, 13.3). Found: C, 57.5; H, 3.9; N, 13.2%; IR (cm^{-1}): 3435, 2067 (SCN^-; ν(CN)), 1595 (ν(C=N)$_{pyridyl}$), 1466, 1105, 1024, 973 (ν(N–O)), 705; for $C_{24}H_{19}CuN_5O_5$ **(2)**: C, 55.3; H, 3.7; N, 13.4. (with 0.5 H_2O: 54.4, 3.8, 13.2). Found: C, 54.7; H, 4.2; N, 12.9%; IR (cm^{-1}): 3440, 1598 (ν(C=N)$_{pyridyl}$), 1466, 1419 (ν$_a$(NO$_2$)), 1299 (ν$_s$(NO$_2$)), 1117, 1025, 971 (ν(N–O)); for $C_{12}H_{10}CuN_2OCl_2$ **(3)**: C, 43.3; H, 3.0; N, 8.4. (with 0.5 H_2O: 42.2, 3.2, 8.2). Found: C, 42.7; H, 3.2; N, 8.5%; IR (cm^{-1}): 3435, 1596 (ν(C=N)$_{pyridyl}$), 1431, 1068, 1023, 960 (ν(N–O)).

[Cu$_3$(PPK)$_3$(μ$_3$–OH)(Cl)$_2$]·nH$_2$O ***(4)***

Compound **4** was obtained according to an alternative method to the one presented in [28], using complex **(3)** for its preparation. [Cu(HPPK)Cl$_2$]$_2$ (3.4 mmol) was dissolved in 50 mL of methanol, and an excess of $(CH_3)_2N–CH_2CH_2–N(CH_3)_2$ (TMEDA) was added, under continuous stirring. The mixture was filtered and dried in air stream. Then, acetone was added, resulting in a green solution with a white precipitate of TMEDA-HCl salt. After filtration, the solution was evaporated to dryness and the dark green residue was dried *in vacuo*. The presence of [Cu$_3$(PPK)$_3$(μ$_3$–OH)(Cl)$_2$]·*n*H$_2$O was confirmed by SCXRD and FT-IR analysis. As indicated by SCXRD, there are big voids present in the structure, occupied partially by water molecules, which do not interact strongly with the host molecule (PLATON estimates the accessible space at 16% of the total cell volume), which causes discrepancies in the elemental analyses. *Anal.* Calc. for $C_{36}H_{28}Cu_3N_6O_4Cl_2$ **(4)**: C, 49.7, H, 3.2, N, 9.7. (with 4H_2O: 45.9, 3.9, 8.9). Found: C, 46.5, H, 4.7, N, 8.7%. IR (cm^{-1}): 3429, 1656 (ν(C=N)), 1597 (ν(C=N)$_{pyridyl}$), 1464, 1121, 1030, 976 (ν(N–O)).

Results and discussion

All complexes are stable in air and dissolve much better in methanol or ethanol than in water. In comparison with the free ketoxime ligand (1591 and 948 cm^{-1}) [30–32], the IR absorption bands such as those for ν(C=N)$_{pyridyl}$ and ν(N–O) groups are slightly shifted towards lower frequencies, for all compounds. The intensity of the acyclic ν(C=N) band from the oxime group, which appears at 1628 cm^{-1} for HPPK, is decreased or covered by other bands after coordination for **1**, **2**, **4,** whereas in **3** this band is visible and is shifted to 1656 cm^{-1}.

Crystal structure of complex 1

The mononuclear, neutral Cu(II) complex **1** crystallizes in the monoclinic $P2_1/c$ space group with one independent molecule in the asymmetric unit—see Fig. 1. The Cu(II) ion shows a distorted square-based pyramidal coordination environment, formed by five N atoms (for geometrical parameters, see Table 2).

The pyridine and imine N atoms originating from two *N*,*N*′-chelating ketoxime and ketoximato ligands, respectively, are situated in the base plane, whereas the N atom coming from the NCS^- anion is located in the apical position. The geometric parameter τ, introduced by Addison et al. [33] as an index of the degree of trigonality for five coordinated systems, indicates quite a high distortion of the geometry around the metal centre, with $\tau = 0.44$ (whereby $\tau = 0$ for a perfect square-based pyramidal geometry). The value of the bond length Cu1–N31 = 2.278(3) Å is rather high in comparison with those reported for Cu(II) complexes with a similar coordination environment. The maximum bond length reported till now is equal to 2.214 Å for 52 hits present in CSD (version 5.37), with a mean value of 1.978 Å. This, as well as the deviation of the NCS^- group from linearity (170.4°), is most probably caused by weak C–H…N (C14–H14…N31^{i} with C…N = 3.498(4) Å, C–H–N = 130°, (i) = x, 1/2 − y, −1/2 + z; C23–H23…N31^{ii}, with C…N = 3.820(3) Å, C–H–N = 162°, (ii) = x, 1/2 − y, 1/2 + z) and C–H…S (C6–H6…S33^{iii} with C…S = 3.685(3) Å, C–

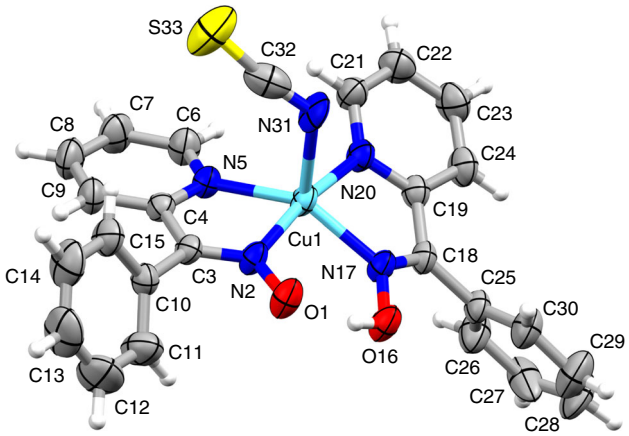

Fig. 1 Molecular structure of **(1)** with displacement ellipsoids drawn at the 50% probability level. The disorder on the phenyl ring C25–C30 is omitted for clarity

Table 2 Selected bond lengths [Å] and angles [°] for **1**

[Cu(HPPK)(PPK)(SCN)] (**1**)			
Cu1–N2	1.970(2)	N2–Cu1–N20	170.78(9)
Cu1–N5	2.048(2)	N2–Cu1–N31	94.20(8)
Cu1–N17	2.004(2)	N5–Cu1–N31	98.21(9)
Cu1–N20	2.005(2)	N17–Cu1–N5	144.30(9)
Cu1–N31	2.278(3)	N17–Cu1–N20	79.87(8)
N2–Cu1–N5	79.79(8)	N17–Cu1–N31	117.20(9)
N2–Cu1–N17	92.51(8)	N20–Cu1–N5	103.37(8)
		N20–Cu1–N31	93.91(8)

* Potential semicoordination, see main text, O31a—symmetry related, (i) = −x, y, ½ − z

H–S = 139°, (iii) = 1 − x, 1 − y, 1 − z; C9–H9···S33^{iv} with C···S 3.588(3) Å, C–H–S = 129°, (iv) = 1 − x, −1/2 + y, 1/2 − z) hydrogen bonds, in which the NCS^- ion and the aromatic rings of the neighbouring molecules are involved. The remaining geometrical parameters stay in good agreement with previous reports. Furthermore, it is worth pointing out that the O atoms from the ketoxime/ato ligands are not coordinated. Both O atoms are involved in many weak C–H···O interactions. These, together with the weak C–H···N and C–H···S hydrogen bonds mentioned before, contribute to the distorted geometry around the metal centre, thereby resulting in an efficiently packed 3D supramolecular assembly.

Up till now, our previous study is the only one dealing with crystal structures of mononuclear Cu(II) complexes with phenyl-2-pyridylketoxime/ato ligands (see Table 3 for the unit cells parameters). Even the molecular structures are pretty much the same (distorted square-pyramidal geometry around the Cu(II) ions, coordination number 5), though the packing of all the compounds differs significantly. It is worth mentioning that the Cu(II) ions in complexes **3** and **4** show a similar type of geometry around the metal ion.

Thermal studies

Thermal analyses of **1**–**4** were carried out to give information about the decomposition processes of the Cu(II) complexes, depending on the counterion involved, nuclearity of the compound and coordination mode of the ketoxime ligand. The summarized results are listed in Table 4.

The decomposition of **1** proceeds in two main stages. The process starts at 150 °C and is completed at 663 °C (Fig. 2a). The first multi-step consists of at least four processes and is connected with a weight loss (WL) of ca. 53%. The second one with a mass loss of ca. 27% consists of two exothermic processes on DTA, namely a weak one at 463 °C and a strong one at 523 °C. The plot of the intensities of volatile species arising during the thermolysis versus time (see ESI, Fig. S1a) **(1)** shows peaks at about 17 and 53 min, corresponding to temperatures of 190 and 550 °C, respectively, which correlates to the most intensive peaks on the DTG curve. At lower temperature, mainly the evolution of CO_2 and H_2O was observed [34]. At this temperature, there are also very weak peaks present, with maxima at 2070/2046 cm^{-1}, originating most likely from the oxime groups [34–37], and at 2239/2204, which could be attributed to the pyridyl ring's decomposition with N_2O release [38]. Spectra registered at higher temperature indicate the release of CO_2 and H_2O. Moreover, a peak occurring in the range of 1300–1400 cm^{-1} could be assigned to SO_2 release, originating from detachment of the NCS^- ion (ESI, Fig. S1c) [39]. Powder diffraction analysis of the residue indicates that CuO is the final product.

In the case of **2**, the thermolysis consists of at least eight overlapping processes (Fig. 2b). The complex is stable up to 94 °C, and no further changes were observed above 392 °C. The result of the TG-IR measurement performed for **2** is presented in Fig. 3. Two distinct peaks appear in the plot of the intensity profiles of the evolved gases (Fig. 3a). At the first stage, the intensity of the peaks is rather low, but the strongest one in the range of 2240–2200 cm^{-1} and the weak one at 1200–1300 cm^{-1} (Fig. 3b) could be evidence of NO_3^- detachment and the formation of nitrogen oxides [39]. The release of NO_2 at this temperature was also apparent from its characteristic smell, noticed upon heating of the compound on the hot stage. The presence of water and carbon dioxide indicates the simultaneous decomposition of the organic ligand.

Table 3 Crystallographic data for known mononuclear [Cu(HPPK)(PPK)X] complexes

X^- Crystal system	Cl^- Monoclinic	CF_3COO^- Monoclinic	$C_3F_7COO^-$ Monoclinic	NCS^- Monoclinic	NO_3^- Orthorhombic
Space group	$P2_1/_n$	$P2_1/c$	$C2/c$	$P2_1/c$	Fdd2
a/Å	9.1844(3)	9.1653(3)	26.798(5)	17.3809(6)	34.7
b/Å	13.7589(5)	17.4582(4)	8.735(5)	8.6465(2)	29.2
c/Å	18.0176(6)	15.5793(4)	22.803(5)	17.4403(5)	8.9
β/°	91.558(3)	97.282(2)	95.343(5)	115.544(4)	

Table 4 Results of thermal analyses of **(1)**–**(3)** in air atmosphere (10°/min)

Compound	Heat effect on DTA	Temperature/°C			Mass loss/%	
		T_i	T_m	T_f	Calc.	Found.
[Cu(HPPK)(PPK)(SCN)] **(1)**	Exo	150	168/185/225/252	343	84.6	80.6
	Exo	435	463/523	663		
[Cu(HPPK)(PPK)(NO_3)] **(2)**	Exo	94	126/129	132	84.7	83.4
	Exo	137	145	–		
	Exo	–	171	–		
	Endo	–	199	–		
	Exo	–	305	–		
	Exo	–	326/329	392		
	Exo	–	348	395		
[Cu(HPPK)Cl_2]$_2$ **(3)**	Endo	180	210	–	76.1	86.6
	Endo	–	216	–		
	Exo	–	221	–		
	Exo	–	260	338		
	Exo	360	375	400		
	Exo	440	731	765		
[Cu_3(PPK)$_3$(μ_3-OH)Cl_2]·$n$$H_2O$ **(4)**	Exo	120	203/209	–	72.5	87.7
	Exo	–	221/227	(270)	*	
	Exo	(270)	346	398		

T_{init} initial temperature, T_{max} maximum temperature, T_f final temperature; * calculated for the unhydrated complex

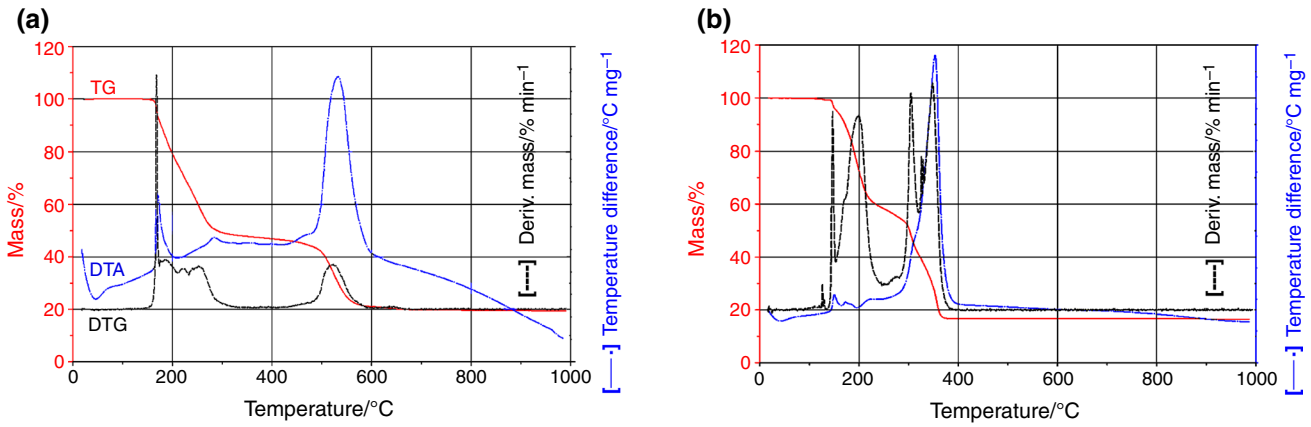

Fig. 2 TG (*red*), DTG (*black*) and DTA (*blue*) curves of **a** [Cu(HPPK)(PPK)(SCN)] **(1)** and **b** [Cu(HPPK)(PPK)(NO_3)] **(2)**

Carbon dioxide and traces of water are the only products registered at higher temperature spectra, whereby a second increase in the intensity of the evolved gases was observed (Fig. 3c).

Thermal decomposition of complex [Cu(HPPK)Cl_2] **3** is also a multi-step process (Fig. 4a). This compound is stable up to 180 °C. Between this temperature and 400 °C, the mass loss is about 39%. The processes occurring at higher temperatures (until ca. 770 °C) are associated with a mass loss of about 48%. The total mass loss of the sample, amounting to 87%, is significantly higher (11%) than calculated for the formation of the CuO residue. This phenomenon can be caused by the intensive evaporation of formed $CuCl_2$ or CuCl, for which the melting points are 498 and 426 °C, respectively [40]. This would also mean that chloride is leaving the compound only at higher temperatures. The measurement was repeated with a heating rate of 5 °C min^{-1}, resulting in a similar mass change (WL = 87.9%). During the TG-IR measurement performed for **3**, the most intensive set of bands was detected at a temperature corresponding to the maximum on the DTG curve above 700 °C, indicating the presence of CO_2 and H_2O.

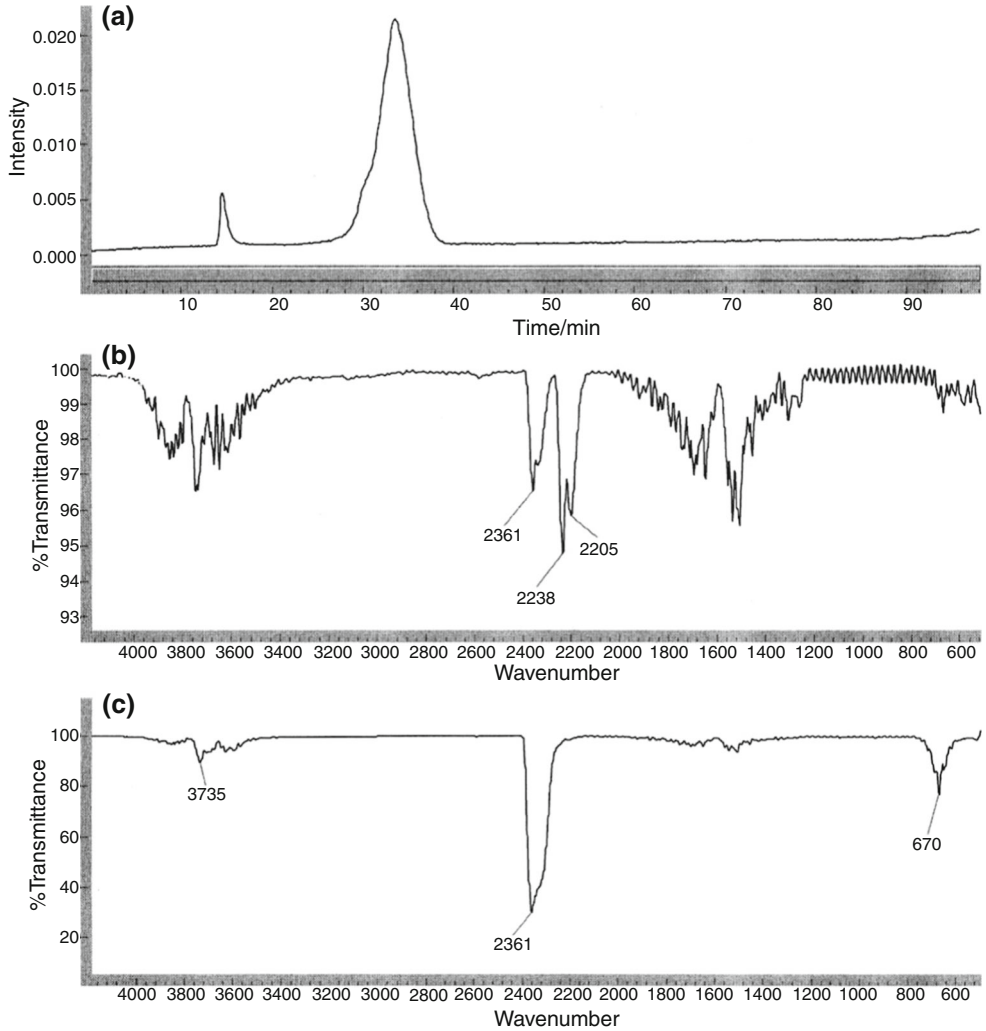

Fig. 3 FT-IR analysis of the volatile products evolved during thermal decomposition of [Cu(HPPK)(PPK)(NO_3)] **(2)**: **a** the intensity of the evolved gases, **b** spectra registered at 160 °C, **c** spectra registered at 350 °C

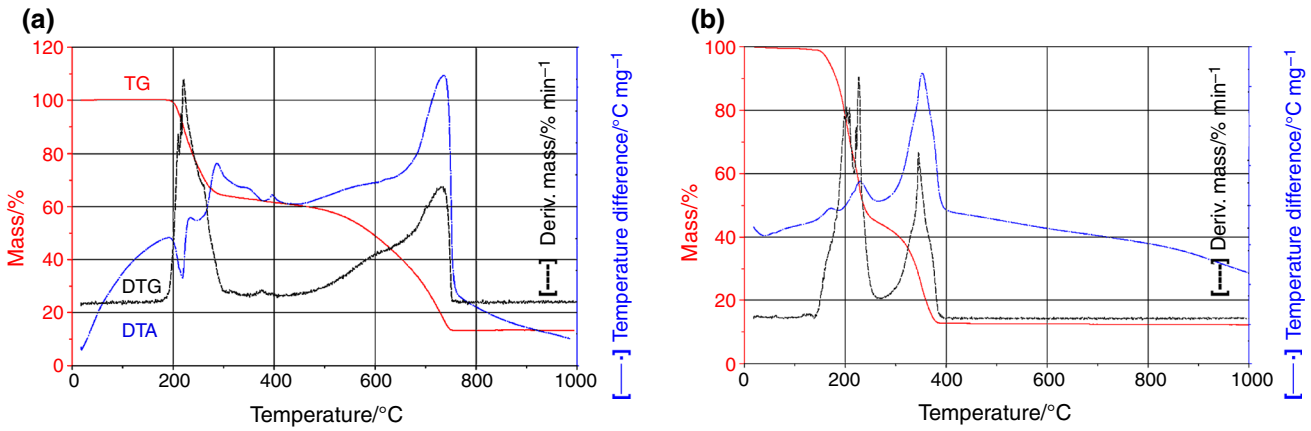

Fig. 4 TG (*red*), DTG (*black*) and DTA (*blue*) curves of **a** $[Cu(HPPK)Cl_2]_2$ **(3)** and **b** $[Cu_3(PPK)_3(\mu_3\text{–}OH)(Cl)_2]\cdot nH_2O$ **(4)**

Complex **4** is thermally stable up to 120 °C, and its decomposition process is connected with three main exothermic effects on the DTA curve, with maxima at 172, 230 and 352 °C (Fig. 4b). In the DTG curve, two main stages are visible. The first one is completed at about 270 °C and connected with a mass loss of ca. 54%. The

second very strong effect, with peak maximum at 346 °C (DTG), is connected with a mass loss of about 32%. The final product is formed at around 400 °C. Similarly to the previous chloride complex, the total mass loss is higher than calculated for the remaining residue of copper oxide (more than 10%). As the decomposition of the compound is finished at much lower temperature than in the case of **3**, the phenomenon could be caused here by the formation and volatilization of double salts of copper chloride that melt below 400 °C [41]. The TG-IR results indicate three maxima in the plot of the intensities of the gas evolution that correspond with temperatures 220, 250 and 360 °C (Fig. 5a). At the first stage of thermolysis, the bands from carbon dioxide show the highest intensity and are followed by medium- and low-intensity peaks situated at 1224, 1180, 1133, 1033 cm^{-1} and 1391, 1338 cm^{-1}, respectively, attributed to HPPK decomposition. At 250 °C, new sharp peaks at 1793 (νC=O) and 1304 cm^{-1} appear in the spectrum, being the volatile products (Fig. 5b), whereas above 360 °C the primary gaseous product is carbon dioxide (Fig. 5c).

Thermal decomposition of the studied complexes in the presence of oxygen takes place for all complexes in two principal steps, leading to the formation of Cu(II) oxide (Fig. S2), which was expected under these conditions, whereas in the case of N_2 atmosphere, the final products can differ and residues such as Cu, CuO or Cu_2O have been observed [42–45]. The thermal stability, as well as the temperature of reaction completion, differs depending on the compound composition [46–48]. For mononuclear complex **1** with NO_3^- counterion, and its previously reported analogous compounds with fluorinated carboxylates, such as CF_3COO^- and $C_3F_7COO^-$, the decomposition process shows a rather similar pattern. The first and second steps of decomposition occur rather close to each other, and the process is finished relatively quickly, namely

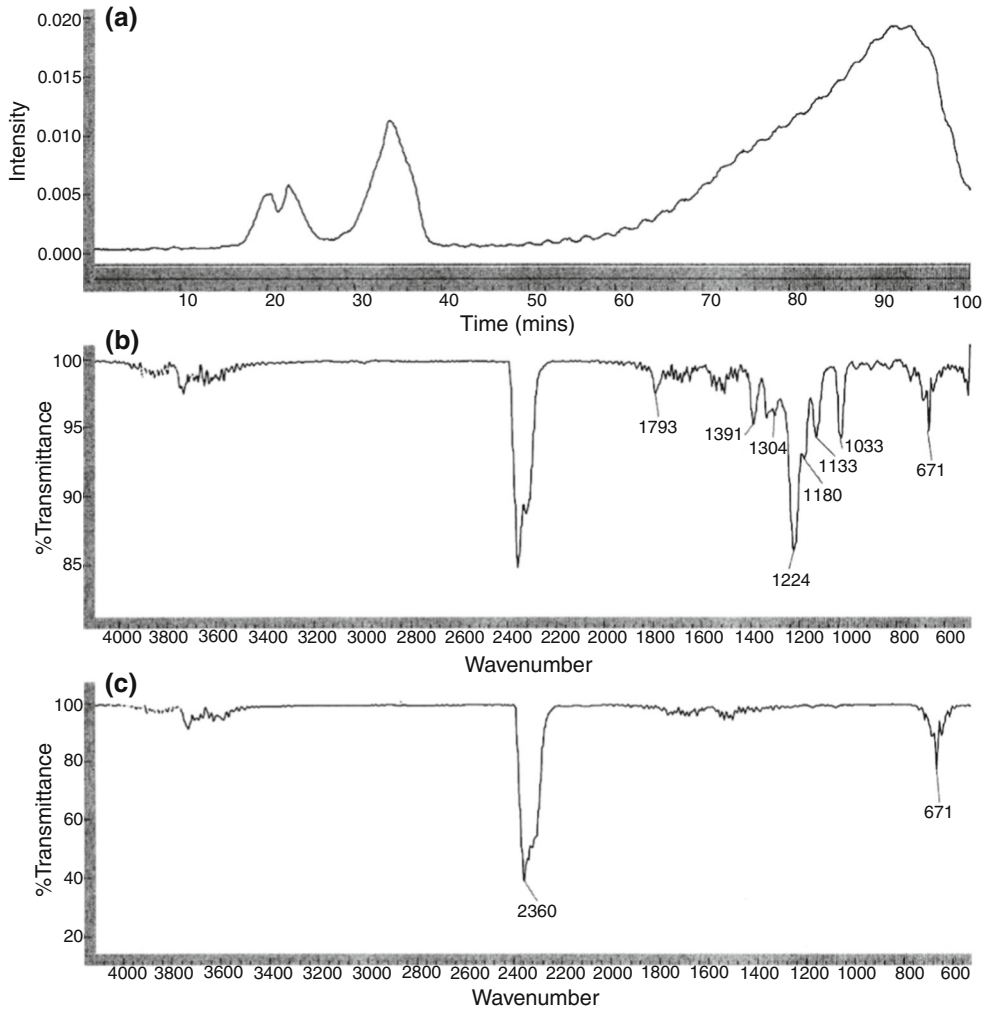

Fig. 5 FT-IR analysis of the volatile products evolving during the thermal decomposition of $[Cu_3(PPK)_3(\mu_3\text{–}OH)(Cl)_2]\cdot nH_2O$ (**4**): **a** the intensity of the evolved gases, **b** spectrum registered at 250 °C, **c** spectrum registered at 360 °C

below 500 °C. It takes a different course in the case of the analogous compounds with Cl^- [15] and NCS^-, whereby the two decomposition steps of are more separated and the process is completed only above 650 °C. It can be assumed that this is due to the presence of the counterions, which in the case of the mononuclear complexes with NO_3^- and fluorinated ions are already being released at the first stage of the decomposition process, whereas in the case of NCS^- and Cl^- ions they are being released during the second stage of the process. Comparing the thermal stability of dinuclear compound **3** and trinuclear copper(II) 9–metallacrown-3 complex **4**, it is clear that the first one is much more stable. The presence of double chloride bridges in **3** can surely be one of the reasons, but also the packing arrangement might have some impact. Whereas the molecules are efficiently packed in **3**, complex **4** is characterized by supramolecular layers, kept together by C–H···π, C–H···Cl and π–π interactions in the *bc* plane, with voids in between, that were initially taken up by solvent molecules (see Fig. S3).

Conclusions

Thermal analyses of a range of copper(II) phenyl-2-pyridylketoxime complexes in dry air atmosphere indicate the influence of counterions and compound composition on the course of the decomposition process. The mononuclear Cu(II) complex **1** (with NCS^-) behaves similarly to a previously reported analogous compound with Cl^-, whereas complex **2** (with NO_3^-) is comparable to analogous complexes with CF_3COO^- and $C_3F_7COO^-$ counterions. The difference is connected with the course of the decomposition, which for the complexes with NCS^- and Cl^- is related to decomposition of the counterions in the second step of the process, whereas NO_3^- and the fluoro-carboxylates are being released in the first step of the process. This is also the reason why the process is finalized faster in the latter case and explains the lack of clear separation between the two decomposition steps, which is apparent for the former. The dinuclear compound **3,** consisting of double chloride bridges, decomposes fully only at 765 °C, meaning at a temperature almost 100 °C higher than observed for the mononuclear compound with monodentate Cl^-, whereas the decomposition of the trinuclear metallacrown **4** is completed at around 400 °C, similarly to the mononuclear compound **2**. The most thermally stable is dinuclear complex **3**, consisting of Cl bridges (ca. 180 °C), then mononuclear compound **1** with NCS^- counterions (ca. 160 °C), followed by trinuclear complex **4** (ca. 150 °C) and mononuclear compound **2** with NO_3^- counterion (ca. 95 °C). Heat treatment under the selected conditions leads to the formation of CuO. Further investigations into this family of compound and their potential applications are ongoing.

Acknowledgements The authors would like to thank the National Science Centre (NCN), Poland for financial support (Grant No. 2013/09/B/ST5/03509).

References

1. Meek TL, Chene GE. The copper(II) syn-phenyl-2-pyridyl ketoxime system part 1. Can J Chem. 1965;43:64–74.
2. Reiner D, Poe DP. Removal of iron, copper, cadmium, cobalt, and nickel from sodium hydroxide by precipitation and extraction with phenyl-2-pyridyl ketoxime. Anal Chem. 1977;49(6):889–91.
3. Liu CH, Liu ChF. Complexes of copper with pyridine-2-aldoxime[1]. J Am Chem Soc. 1961;83:4169–72.
4. Banerjea DK, Tripathi KK. Spectrophotometric determination of iron and copper with methyl-2-pyridyl ketoxime and their simultaneous determination in mixtures. Anal Chem. 1960;32(9):1196–200.
5. Milios CJ, Stamatatos TC, Perlepes SP. The coordination chemistry of pyridyl oximes. Polyhedron. 2006;25:134–94.
6. Robertson D, Cannon JF, Gerasimchuk N. Double-stranded metal-organic networks for one-dimensional mixed valence coordination polymers. Inorg Chem. 2005;44(23):8326–42.
7. Milios CJ, Kefalloniti E, Raptopoulou CP, Terzis A, Escuer A, Vicente R, Perlepes SP. 2-Pyridinealdoxime (py)CHNOH in manganese (II) carboxylate chemistry: mononuclear, dinuclear, tetranuclear and polymeric complexes, and partial transformation of (py)CHNOH to picolinate (–1). Polyhedron. 2004;23:83–95.
8. Smith AG, Tasker PA, White DJ. The structures of phenolic oximes and their complexes. Coord Chem Rev. 2003;241:61–85.
9. Goldcamp MJ, Robison SE, Krause JA, Baldwin MJ. Oxygen reactivity of a nickel(II)-polyoximate complex. Inorg Chem. 2002;41(9):2307–9.
10. Chaudhuri P. Homo- and hetero-polymetallic exchange coupled metal-oximates. Coord Chem Rev. 2003;243:143–90.
11. Afrati T, Dendrinou-Samara C, Raptopoulou C, Terzis A, Tangoulis V, Kessissoglou DP. Copper inverse-9-metallacrown-3 compounds showing antisymmetric magnetic behaviour. Dalton Trans. 2007;(44):5156–64.
12. Guang-Xiang L, Huan-Min X, Xiao-Ming R. Synthesis, crystal structure and magnetic properties of a novel copper inverse-9-metallacrown-3 complex. Chin J Struct Chem. 2010;29(7):1072–6.
13. Akine S, Taniguchi T, Saiki T, Nabeshima T. Ca^{2+}- and Ba^{2+}-selective receptors based on site-selective transmetalation of multinuclear polyoxime-zinc(II) complexes. J Am Chem Soc. 2005;127(2):540–1.
14. Afrati T, Pantazaki AA, Dendrinou-Samara C, Raptopoulou C, Terzis A, Kessissoglou DP. Copper inverse-9-metallacrown-3 compounds interacting with DNA. Dalton Trans. 2010;39:765–75.
15. Szczęsny R, Muzioł TM, Gregory DH, Szłyk E. Structural and thermal characterization of copper(II) complexes with phenyl-2-pyridylketoxime and deposition of thin films by spin coating. Chem Pap. 2015;69(4):569–79.

16. Vogh JW. Isolation and analysis of carbonyl compounds as oximes. Anal Chem. 1971;43(12):1618–23.
17. Salonen M, Saarinen H, Orama M. Formation of Zinc(II) and Cadmium(II) complexes with pyridine oxime ligands in aqueous solution. J Coord Chem. 2003;56(12):1041–7.
18. Salonen M, Saarinen H, Orama M. Formation of cobalt(II) complexes with five pyridine oximes in aqueous solution. J Coord Chem. 2005;58(4):317–26.
19. Chakravorty A. Structural chemistry of transition metal complexes of oxime. Coord Chem Rev. 1974;13:1–46.
20. Hudák A, Košturiak A. Preparation, IR characterization and thermal properties of some metal complexes of isatin-3-oxime. J Therm Anal Calorim. 1999;58:579–87.
21. Prathapachandra Kurup MR, Chandra SV, Muraleedharan K. Synthesis, spectral and thermal studies of o-vanillin oxime complexes of Zinc(II), Cadmium(II) and Mercury(II). J Therm Anal Calorim. 2000;61:909–14.
22. Prathapachandra Kurup MR, Lukose E, Muraleedharan K. Synthesis, characterization and thermal studies of some iron(III) complexes of o-vanillin oxime. J Therm Anal Calorim. 2000;59:815–25.
23. CrysAlis CCD. Oxford Diffraction Ltd. England: Abingdon; 2000.
24. CrysAlisPro RED, Agilent Technologies, Version 1.171.35.21 (release 20-01-2012 CrysAlis171.NET).
25. Sheldrick GM. A short history of SHELX. Acta Crystallogr Sect A. 2008;64:112–22.
26. Macrae CF, Bruno IJ, Chisholm JA, Edgington PR, Mc-Cabe P, Pidcock E, Rodriguez-Monge L, Taylor R, van de Streek J, Wood PA. Mercury CSD 2.0—new features for the visualisation and investigation of crystal structures. J Appl Crystallogr. 2008;41:466–70.
27. Xiang J, Li Q, Mei P. Di-μ-chloro-bischloro(phenyl 2-pyridyl ketone oxime κ2 *N,N′*)copper(II). Acta Cryst. 2006;E62:m2348–9.
28. Li R, Lu J, Li D, Cheng S, Dou J. Syntheses, structures, in vitro cytotoxicities and DNA-binding properties of four copper complexes based on a phenyl 2-pyridyl ketoxime ligand. Trans Met Chem. 2014;39(5):507–17.
29. Mohan M, Paramhans BD. Transition metal chemistry of oxime-containing ligands, part XI. Copper(II) complexes of syn-phenyl-2-pyridylketoxime and syn-methyl-2-pyridylketoxime. Trans Met Chem. 1980;5:113–7.
30. Stamatatos ThC, Bell A, Cooper P, Terzis A, Raptopoulou CP, Heath SL, Winpenny REP, Perlepes SP. Old ligands with new coordination chemistry: linear trinuclear mixed oxidation state cobalt(III/II/III) complexes and their mononuclear "ligand" cobalt(III) complexes featuring 2-pyridyloximates. Inorg Chem Commun. 2005;8:533–8.
31. Stamatatos ThC, Diamantopoulou E, Tasiopoulos A, Psycharis V, Vincente R, Raptopoulou CP, Nastopoulos V, Escuer A, Perlepes SP. Enneanuclear Ni(II) complexes from the use of the flexible ligand 2-pyridinealdoxime: the nature of the inorganic anion does not affect the chemical and structural identity of the cationic cluster. Inorg Chim Acta. 2006;359:4149–57.
32. Afrati T, Zaleski CM, Dendrinou-Samara C, Mezei G, Kampf JW, Pecoraro VL, Kessissoglou DP. Di-2-pyridyl ketone oxime in copper chemistry: di-, tri-, penta- and hexanuclear complexes. Dalton Trans. 2007;(25):2658–68.
33. Addison AW, Rao TN, Reedijk J, van Rijn J, Verschoor GC. Synthesis, structure, and spectroscopic properties of copper(II) compounds containing nitrogen–sulphur donor ligands; the crystal and molecular structure of aqua1,7-bis(N-methylbenzimidazol-2′-yl)-2,6-dithiaheptanecopper(II) perchlorate. J Chem Soc Dalton Trans. 1984;(7):1349–56.
34. Madarász J, Pokol G. Comparative evolved gas analyses on thermal degradation of thiourea by coupled TG-FTIR and TG/DTA-MS instruments. J Therm Anal Calorim. 2007;88(2):329–36.
35. Nakamoto K. Infrared and Raman Spectra of inorganic and coordination compounds: part A: theory and applications in inorganic chemistry. 6th ed. New York: Wiley; 2009. p. 287–8.
36. Ge M, Ma C, Tong S, Xue W, Pu Z, Wang D. Molecular and electronic structures of acryloyl isothiocyanate, CH_2=CHC(O)NCS: a joint experimental and theoretical study. New J Chem. 2009;33:2155–61.
37. Durig JR, Sullivan JF, Durig DT, Cradoc N. Infrared spectra of some matrix isolated organoisothiocyanate molecules. Can J Chem. 1985;63:2000–6.
38. Zhang Z, Wang G, Luo N, Huang M, Jiu M, Luo Y. Thermal decomposition of energetic thermoplastic elastomers of poly(glycidyl nitrate). J Appl Polym Sci. 2014;131:40965.
39. Jiang X, Li C, Wang T, Liu B, Chi Y, Yan J. TG-FTIR study of pyrolysis products evolving from dyestuff production waste. J Anal Appl Pyrolysis. 2009;84:103–7.
40. Burgelman M, De Vos A. Evaporation of CuCl and $CuCl_2$ for the fabrication of Cu_2S/CdS thin-film solar-cells. Thin Solid Films. 1983;102(4):367–74.
41. Seiyama T. New horizons in catalysis: part 7B. In: Proceedings of the 7th international congress on catalysis, Tokyo, 30 June-4 July 1980 (Studies in surface science and catalysis). Amsterdam: Elsevier; 1981. p. 819.
42. Radovanovic BS, Premovic PI. Thermal behaviour of Cu(II)-urea complex. J Therm Anal. 1992;38(4):715–9.
43. Sceney CG, Hill JO, Magee RJ. Thermal analysis of copper dithiocarbamates. Thermochim Acta. 1975;11:301–6.
44. Prasad R. Mechanism and kinetics of thermal decomposition of ammoniacal complex of copper oxalate. Thermochim Acta. 2003;406:99–104.
45. Nasui M, Mos RB, Petrisor T Jr, Gabor MS, Varga RA, Ciontea L, Petrisor T. Synthesis, crystal structure and thermal decomposition of a new copper propionate $Cu(CH_3CH_2COO)_2{\cdot}2H_2O$. J Anal Appl Pyrolysis. 2011;92:439–44.
46. Bartyzel A. Synthesis, thermal study and some properties of N_2O_4—donor Schiff base and its Mn(III), Co(II), Ni(II), Cu(II) and Zn(II) complexes. J Therm Anal Calorim. 2016. doi:10.1007/s10973-016-5804-0.
47. Olar R, Badea M, Ferbinteanu M, Stanica N, Alan I. Spectral, magnetic and thermal characterization of new Ni(II), Cu(II), Zn(II) and Cd(II) complexes with a bischelate Schiff base. J Therm Anal Calorim. 2016. doi:10.1007/s10973-016-5433-7.
48. Emam SM, AbouEl-Enein SA, Emara EM. Spectroscopic studies and thermal decomposition for (bis-((E)-2-(4-ethylphenylimino)-1,2-diphenylethanone) Schiff base and its Co(II), Ni(II), Cu(II), Zn(II) and Cd(II) complexes prepared by direct and template reactions. J Therm Anal Calorim. 2016. doi:10.1007/s10973-016-5835-6.